Effective Thermo-Capillary Mixing in Droplet Microfluidics Integrated with a Microwave Heater

Gurkan Yesiloz,[†] Muhammed S. Boybay,[†,‡] and Carolyn L. Ren*[,†]

[†]Department of Mechanical and Mechatronics Engineering, University of Waterloo, 200 University Avenue West, Waterloo, Ontario N2L 3G1, Canada

[‡]Department of Computer Engineering, Antalya International University, Universite Caddesi No:2, 07190 Antalya, Turkey

Supporting Information

ABSTRACT: In this study, we present a microwave-based microfluidic mixer that allows rapid mixing within individual droplets efficiently. The designed microwave mixer is a coplanar design with a small footprint, which is fabricated on a glass substrate and integrated with a microfluidic chip. The mixer works essentially as a resonator that accumulates an intensive electromagnetic field into a spiral capacitive gap (around 200 μm), which provides sufficient energy to heat-up droplets that pass through the capacitive gap. This microwave actuation induces nonuniform Marangoni stresses on the interface, which results in three-dimensional motion inside the droplet and thus fast mixing. In order to evaluate the performance of the microwave mixer, droplets with highly viscous fluid, 75% (w/w) glycerol solution, were generated, half of which were seeded with fluorescent dye for imaging purposes. The relative importance of different driving forces for mixing was evaluated qualitatively using magnitude analysis, and the effect of the applied power on mixing performance was also investigated. Mixing efficiency was quantified using the mixing index, which shows as high as 97% mixing efficiency was achieved within the range of milliseconds. This work demonstrates a very unique approach of utilizing microwave technology to facilitate mixing in droplet microfluidics systems, which can potentially open up areas for biochemical synthesis applications.

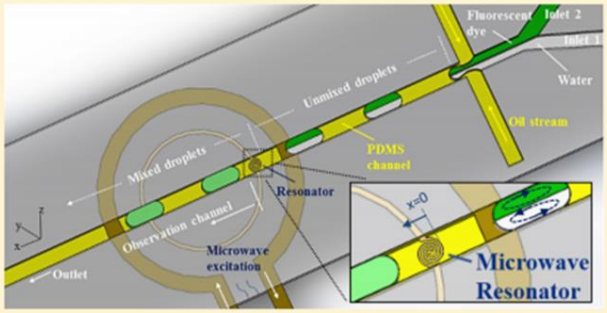

In many microfluidic applications rapid, on-demand mixing is crucial because of the need for homogenization of multiple reagents in biochemical reactions, drug discovery, and synthesis of nucleic acids, as well as dissolving enzymes and proteins in liquids where analysis take place.[1,2] However, mixing in microfluidics is challenging due to its laminar flow nature and is often dominated by molecular diffusion. For this reason, many strategies have been reported[3−5] to enhance mixing using different methods as outlined in recent review articles.[6,7]

In general, microfluidic mixing mechanisms can be classified as active and passive methods. Active techniques utilize external forces to perturb the fluid flow, and passive techniques rely on particular microchannel designs to increase contact time or area between different reagents.[7,8] Most passive mixing methods employ one or a combination of several of the following techniques: splitting-and-recombination, chaotic advection, serial and parallel lamination, serpentine channels, injection, and droplets.[9,10] Although passive methods operate without the need for additional external components, they have limitations such as long mixing lengths (>a few centimeters), which may result in unmixed regions and low efficiency for mixing highly viscous fluids.[10,11] In addition, fabrication of such mixers likely experience higher risks for failure due to their complex channel configurations. In contrast, active methods have the potential to overcome these limitations with the cost of incorporating active control components to induce external disturbance to the flow. Common active methods for microfluidic mixing include dielectrophoresis,[12,13] electro-kinetics,[14−16] magneto-hydrodynamics,[17−20] thermal,[21,22] pressure,[23,24] and acoustics.[25−29] Despite the success of various active mixing methods, there are still challenges for achieving rapid mixing, usually limited by the actuation and response time of the system.[11] Effective mixing of highly viscous fluids often requires increasing the magnitude of the external source and thus power consumption.[11] Integration of active control components with a single microfluidic chip also remains a challenge as well due to relatively large system footprints.

It is well-known that rapid mixing can be achieved in droplet microfluidics because of the three-dimensional (3D) flow occurring within them.[30] However, 3D flow only occurs within each half of the droplet[31−33] if they are traveling through straight channels, and mass transfer in the transversal direction still relies on molecular diffusion as shown by the measured flow pattern in droplets using particle image velocimetry (PIV) techniques.[31] Boybay et al.[34] attempted to employ microwave heating to mix two halves of a droplet, one-half filled with

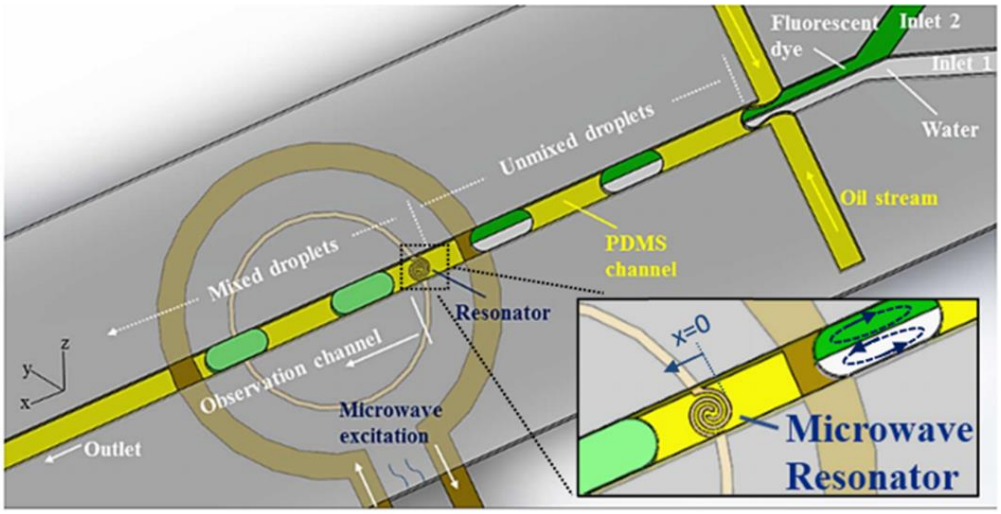

Figure 1. Schematic description of the microfluidic mixer.

fluorescent dye and the other pure water, but failed unfortunately because the symmetric double T design of the capacitive gap was not able to generate massive nonuniform temperature gradients within the droplets. As a result, the induced marangoni stresses were not strong enough to induce disturbance to the flow field and thus enhance cross-stream mixing. In addition, a passivation layer of hard polydimethylsiloxane (PDMS) was used between the heater and the working fluid, which was a few micrometers thick. Such a thick layer likely reduces heat deposition within the droplets and thus the induced temperature gradients and flow disturbance. Mixing of the reagents within the entire droplet is usually realized by pumping it through serpentine channels,[35] which induces 3D flow within the entire droplet, or by agitating it using active means such as laser or acoustic wave. With the promising potential of droplet microfluidics as enabling tools for high-throughput analysis, developing methods to achieve rapid mixing within droplets without the need for long or serpentine channels is important.

In this study, we present a microwave-based thermocapillary microfluidic mixer that enables almost instantaneous mixing, requires simple integration with microfluidic devices, and consumes less than 0.5W of power. We demonstrated its excellent performance in mixing highly viscous fluids within nanoliter-sized droplets. More importantly, this microwave mixer can also trigger and initiate reactions at the same time of mixing using the microwave energy. This work demonstrates a very unique approach of utilizing microwave sensor technology to facilitate microfluidics mixing.

■ EXPERIMENTAL SECTION

The experimental setup consists of a microfluidic chip integrated with a microwave resonator, which is the heater as well, a microwave signal generator (HMC-T2100, Hittite), a vector network analyzer (VNA) (MS2028C, Anritsu), a fluid pumping unit (Fluigent MFCS-8C), and an inverted microscope (Eclipse Ti, Nikon) equipped with a CCD camera (Q-imaging). The schematic description of the integrated mixer unit is demonstrated in Figure 1, where the microwave heater is a concentric ring structure with the outer ring excited at a desired operating frequency and provided with power through the signal generator and the inner ring resonating accordingly. The signal generator was controlled via a computer, and the VNA was used to characterize the microwave resonator. Droplets were generated using a flow focusing generator where the continuous phase is a fluorinated oil, FC-40 (Sigma-Aldrich), and the dispersed phase consists of an aqueous solution and the same solution seeded with fluorescent dye. These two liquid solutions were flowing side by side before reaching the generator and then form droplets half by half. The aqueous solution was varied from pure water to a highly viscous liquid, 75% (w/w) glycerol solution, with a viscosity of 22.7 mPas at 20 °C. A Y-channel design was used to generate the side-by-side dispersed flow streams. Fluorescent dye, Thioflavin S (ThS) (Sigma-Aldrich), was used to seed one of the flow streams, and the mixing performance was evaluated using the fluorescent images obtained through the microscope and CCD camera. The acquired images were processed using ImageJ (National Institute of Health, MD, U.S.A.).

Device Fabrication. The mixing device consists of a PDMS mold with the designed microchannels for droplet generation and transport and a microwave sensor; a glass base with the microwave components. On top of the microwave sensor is a thin layer of SiO_2, which was coated on the sensor using magnetron sputtering (AJA Orion 5) techniques. This layer was designed to prevent direct contact between the working fluids and metal-made sensor to avoid any contamination. Its thickness is around 500 nm, which is estimated using the protocol of the sputtering system. The electrical traces for the microwave components were fabricated using a combination of photolithography and electroplating.

Briefly, the positive photoresist, S1813 (Rohm-Haas), was spin-coated at 1500 rpm for 60 s onto a 50 nm thick copper film (EMF Corporation) that had been predeposited on a glass slide and then baked at 95 °C for 120 s. The design was patterned into the photoresist via UV lithography and subsequently developed with MF-319 (Rohm-Haas) for 2 min. The patterned slide is then immersed in an acidic copper electroplating solution (0.2 M $CuSO_4$, 0.1 M H_3BO_3, and 0.1 M H_2SO_4) and electroplated at 2 mA for 5 min and 4 mA for 10 min.[36] After electroplating, the photoresist was removed with acetone leaving an electroplated copper film approximately 2

μm thick. Next, the base layer of predeposited copper was removed by etching with dilute ferric chloride (5%) (MG Chemicals). SiO_2 was deposited on top of it. A subminiature version A (SMA) connector (Tab Contact, Johnson Components) was then soldered to the electrodes of the microwave components to provide an external connection to the microwave signal generator.

For the fabrication of microfluidic chips, SU-8 masters were fabricated on silicon wafers using the same soft-lithography technique developed previously.[37] In order to make PDMS replica molds, PDMS prepolymer was mixed at a 10:1 ratio of base to curing agent, degassed, and molded against the SU-8/silicon master and then cured at 95 °C for 2 h. The molds were then peeled off from the master, and fluidic access holes were made using a 1.5 mm biopsy punch. Both the finished microwave components and the PDMS mold were then treated with oxygen plasma at 29.7 W, 500 mTorr for 30 s. The plasma treatment process renders PDMS hydrophilic; however, for generating water in oil droplets stably, the PDMS channels need to be hydrophobic which was realized by coating Aquapel (PPG Industries) onto the channel surface.

Mixing Mechanism. The working principle of the microwave-microfluidic mixing device is shown in Figure 1. Droplets are transported through a straight microchannel. Two symmetric counter-rotating recirculation zones are formed in each half of the droplet provided no external disturbance, which creates a barrier limiting the mixing between the two halves through diffusion. The flow topology and internal dynamics inside droplets were studied in detail elsewhere[32,33] using μ-PIV techniques. Complete mixing could occur when these two halves are agitated in the cross-stream direction. The essential element and main trigger of the mixing, herein, is the localized microwave heater, which works as a microwave resonator fundamentally.

The resonator structure is made of two concentric copper loops similar to the one presented previously.[36,38] Microwave signal is excited via the outer coplanar transmission line loop, which supplies a time-varying oscillating current circulating around the loop and a magnetic field passing through the loop. The inner loop with a small gap constructs the resonator and the microchannel where droplets are passing through is aligned on top of this gap perpendicularly. Microwave energy is inductively coupled to the resonator by the excitation loop, and there is no physical contact between the two loops. In this microwave structure, the electric field energy is stored within the capacitor of the resonator (the spiral region), and the magnetic field energy is stored in the inductor of the resonator (the inner loop). When there is a perturbation in the permittivity of the medium, the resonance frequency of the microwave structure shifts. For example, when a droplet with aqueous solutions enters the resonator region, it causes a shift in the operating frequency because of its different electrical properties from those of the continuous oil phase. This shift could be used to sense the droplet content and heat the droplet if power is supplied to the resonator only at the shifted frequency associated with the droplet content. After the droplet completely leaves the resonator region, the operating frequency shifts back to that associated with the oil, and no energy is received. Therefore, the microwave heating is self-triggered, remote, and selective.

The electrical field in the resonator region is three-dimensionally nonuniform, as shown in Figure 2, which is a numerical prediction using a commercial software, Ansys HFSS.

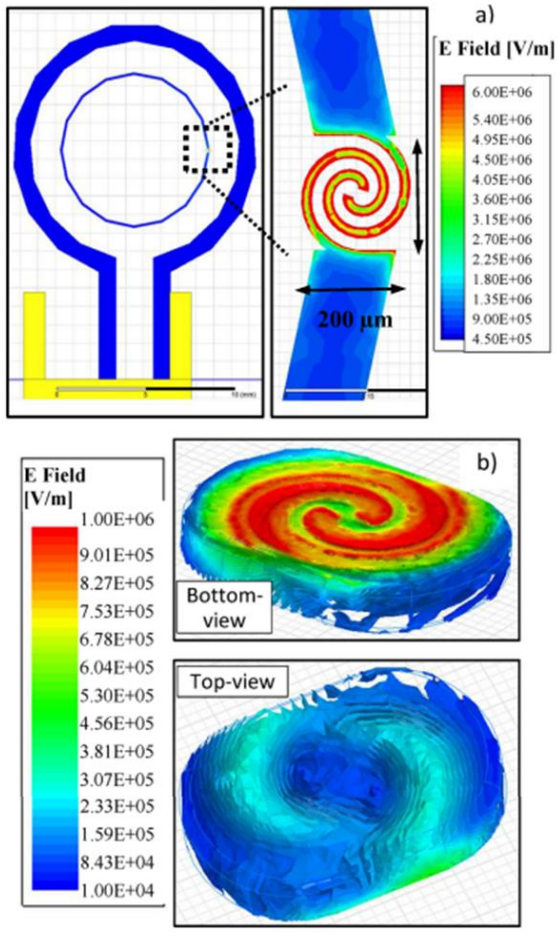

Figure 2. Operating mechanism of the microfluidic mixer and nonuniform electrical field distribution inside droplet.

It can be seen that the spiral region has a high and intense E field, and the rest of the structure holds a very weak E field, which is negligible in comparison to the spiral. The high electric field results in concentrated dielectric heating within the droplet when it is passing through the gap region. The relationship between the deposited energy within the droplet and the electrical field intensity can be described as

$$P = \omega \varepsilon_0 \varepsilon'' |E|^2 \quad (1)$$

where ω is the angular frequency, ε_0 the permittivity of vacuum, ε'' the imaginary part of the relative permittivity, and E the electric field intensity. For further analysis, the distribution of volume loss density inside droplet and the electric field at different magnitudes can be found in Supporting Information (SI) (Figure S1 and Figure S2, respectively).

The nonuniform energy distribution within droplets results in nonuniform temperature distribution which induces spatial variation in fluid properties such as density, viscosity, diffusion coefficient, and interfacial tension. The temperature-dependent fluid properties induce cross-streamflow enhancing 3D mixing within droplets. In general, when a droplet is passing through a straight channel without any external disturbance, the cross-stream mixing is suppressed because the symmetries in the flow creates invariant surfaces that serve as barriers preventing cross-stream mixing.[4,39] Grigoriev et al.[4] presented a theoretical analysis on the existence of invariant surfaces inside droplets

and reported that the presence of chaotic advection *does not* guarantee a full mixing, which requires a mechanism to destroy the symmetry (flow invariant). The microwave induced spatially nonuniform temperature distribution over the entire droplet overcomes symmetries resulting in 3D mixing. Moreover, the motion of droplet dynamically influence the electrical field which further enhances the chaotic motion and thus mixing within the droplet.

The mixing mechanism is a complex phenomenon involving the understanding of nonuniform electrical field, nonuniform energy distribution within droplets, and their strong dynamic coupling, which is beyond the scope of this study. In order to shed light on the mixing mechanism, magnitude analysis on the influencing parameters is performed using the Buckingham Pi theorem.[40−42] Mixing index (MI), which indicates the mixing efficiency is influenced by both the fluid properties and operating conditions, can generally be described as

$$\mathrm{MI} = f(P_{\mathrm{exc}}, \gamma, U_{\mathrm{d}}, \mu, \rho, \alpha, D_{\mathrm{dif}}, L_{\mathrm{d}}, L_{\mathrm{cw}}, L_{\mathrm{h}}, L_{\mathrm{dis}}) \quad (2)$$

where P_{exc} [W] denotes the microwave excitation power; γ [N/m] the interfacial tension; U_{d} [m/s] the droplet velocity; μ [mPa s], ρ [kg/m^3], and α [m^2/s] the dynamic viscosity, density, and thermal diffusivity of the droplet material respectively; D_{dif} [m^2/s] the diffusion coefficient of the fluorescent dye; L_{d} [m], L_{cw} [m], and L_{h} [m] the droplet length, width, and height respectively; and L_{dis} [m] the distance that a droplet needs to travel to achieve homogenization. In this study, droplet generation was in the squeezing regime[37] where droplets are filled almost the entire cross-section of the channel leaving a very thin film (~2% of channel width) of the continuous phase between the droplets and channel walls. Therefore, the droplet width and height are also representing the channel width and height. Detailed derivations of the dimensionless groups can be found in SI-S3. Briefly, by choosing the viscosity, diffusion coefficient and droplet width as the repeating parameters to nondimensionalize the rest of the parameters, the dimensionless mixing index can be described as

$$\mathrm{MI} = f(P^*_{\mathrm{exc}}, \gamma^*, \mathrm{Sc}, \mathrm{Pe}, \mathrm{Le}, L^*_{\mathrm{c}}, L^*_{\mathrm{d}}, L^*_{\mathrm{dis}}) \quad (3)$$

where $P^*_{\mathrm{exc}} = \frac{P_{\mathrm{exc}} L_{\mathrm{cw}}}{\mu {D_{\mathrm{dif}}}^2}$, $\gamma^* = \frac{(\gamma 0 - \gamma) L_{\mathrm{cw}}}{\mu \alpha}$, $\mathrm{Pe} = \frac{U_{\mathrm{d}} L_{\mathrm{cw}}}{D_{\mathrm{dif}}}$,

$$\mathrm{Sc} = \frac{\mu}{\rho D_{\mathrm{dif}}}, \mathrm{Le} = \frac{\alpha}{D_{\mathrm{dif}}}, L^*_{\mathrm{d}} = \frac{L_{\mathrm{d}}}{L_{\mathrm{cw}}}, L^*_{\mathrm{c}} = \frac{L_{\mathrm{ch}}}{L_{\mathrm{cw}}}, L^*_{\mathrm{dis}} = \frac{L_{\mathrm{dis}}}{L_{\mathrm{cw}}}$$

Herein, Pe, Sc, and Le stand for Peclet number, Schmidt number, and Lewis number, respectively. For a given set of geometric and flow conditions, droplet size can be considered uniform. The main focus would then be evaluating the relative importance of different driving forces for mixing. Considering the ThS dye with a nominal radius of 0.4 nm in the glycerol solution (75% w/w) with a dynamic viscosity of 22.7 [mPas], its diffusion coefficient can be estimated as 2.27×10^{-11} [m^2/s] at 22 °C,[43] which could increase to 2.06×10^{-10} [m^2/s] when temperature is increased to 87 °C. For the power used in this study ranging from 24−27 dbm (0.25 to 0.50 W), the measured temperature change above room temperature of 22 °C ranged from 47 to 65 °C (please see SI, Figure S4) which results in the highest temperature of 87 °C. Based on this temperature range, the Sc number which indicates the competition between viscous and mass diffusivity ranged from 7.93×10^5 to 1.49×10^4 meaning that viscous diffusivity is more important. Similarly, the Pe number which indicates the competition between convection and mass diffusion ranged from 2196 to 251 suggesting that convection is more dominant than mass diffusion, and the Lewis number that indicates the relative importance between thermal and mass diffusion ranged from 3805 to 358 suggesting that thermal diffusion is dominant over mass diffusion. Comparing these three numbers, viscous diffusion is relatively more dominant than the others. By examining the dimensionless interfacial tension which indicates the competition between interfacial tension and viscous and thermal diffusivities, it is found that it varies from almost zero when no heating to ~4500 with the maximum heating. It suggests when temperature increases, interfacial tension force is mainly dominant over all the other driving forces. The thermally induced interfacial tension gradient results in a strong Marangoni (thermocapillary) effect over the droplet interface that causes the interface to be torn in a massive, 3D manner.[3,44] As a result, 3D flow is induced within the droplet which leads to almost instantaneous mixing as shown in Figure 3.

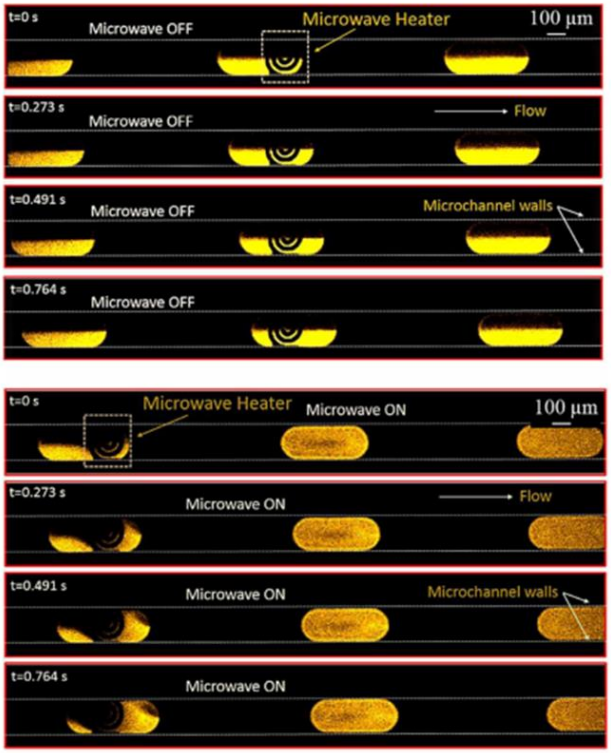

Figure 3. Droplets are moving and passing over the microwave heater. Microwave heating initiates mixing between the two halves and agitates flow pattern inside the droplet, which helps stirring the two halves of the droplet.

RESULTS AND DISCUSSION

To demonstrate the mixing efficiency of the microwave-based microfluidic mixer, droplets with half doped with ThS dye are generated in a straight microchannel, where the channel width and height are fixed to be 200 um and 50 um, respectively. As illustrated in Figure 1, a combination of Y-channel and flow focusing design was used to form the droplets where the two fluid inlets from the Y-channel form the dispersed phase and a perpendicular oil stream serving as the continuous phase pinches off droplets. In the experiments, fluids were pumped through a pressure system. As mentioned earlier, most active

mixing methods are based on hydrodynamic disturbance of flow which is not very effective for mixing highly viscous fluids such as the situation considered in this study.[46,10] In order to demonstrate its mixing performance, both pure water and highly viscous 75% (w/w) glycerol solutions were used as the continuous phase. Figure 3 shows the mixing of droplets with the glycerol solution when they are passing by the microwave resonator at different time lapses under the on/off scenarios of the microwave resonator. Cross-stream mixing between the two halves of droplets is negligible when the microwave resonator is off while mixing is almost instantaneous when the microwave resonator is on. Microwave assisted mixing for pure water and pure water seeded with ThS dye is more efficient due to its low viscosity as shown in Figure S6 in SI.

As discussed by Muradoglu and Stone,[2] and Wiggins and Ottino,[45] the required condition to produce chaotic advection is to have time-dependent cross-streamflow motion. As seen in Figure 3, while the droplet enters the resonator region and starts receiving energy, the dye in the front region is pulled cross the flow stream toward the upper half of the droplet by following the resonator shape. This stirring phenomena should occur in the height direction as well as suggested by the nonuniform electrical field in this direction shown in Figure 2. It is also noted that while mixing is happening in the front region, the back of the droplet is almost unaffected since it is not being heated yet. As droplet keeps sweeping through the resonator region, the time-varying Marangoni effect induces 3D motion over the entire droplets resulting in chaotic mixing. A video showing the microwave agitation event with the comparison of the resonator being on and off can be found in SI (video S1). Quantitative analysis of mixing was also done by measuring the fluorescent intensity profiles of the images. In Figure 4, the intensity profiles across the droplet width before

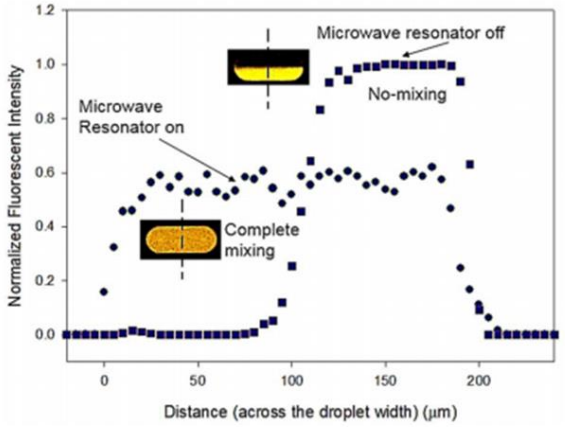

Figure 4. Mixing in the absence and presence of microwaves.

and after mixing are denoted. The image showing complete mixing is taken from the third droplet in Figure 3. It is clearly seen that the fluorescent intensity is relatively homogeneous across the entire droplet width.

It should be noted that rapid mixing is difficult to obtain in microfluidics, which could take a significantly longer time than the microwave-assisted mixer presented here. For example, the mixing time driven by pure diffusion can be estimated by $t_D \approx l^2/D$, where t_D is the time elapsed since diffusion starts, l the characteristic length which could be considered as the channel width in this study as diffusion occurs between two halves of the droplets that are aligned side-by-side in the width direction, and D the diffusion coefficient of the fluorescent dye, ThS. Then the time scale to reach full mixing is estimated as 1762 s considering l = 200 μm and $D = 2.27 \times 10^{-11}$ m^2/s, which is 3 orders of magnitude longer than the mixing time achieved here (i.e., less than 1 s). Although mixing occurs almost instantaneously when a droplet enters the resonator region, thorough mixing is achieved after the droplet travels a few hundred micrometers away from the resonator, as shown in Figure 3. When temperature increases, which can be achieved by increasing the input power to the resonator, the Marangoni effect is stronger and should result in faster mixing. In other words, thorough mixing could occur within a shorter distance when the input power is higher. In order to quantitatively investigate the effect of the input power on mixing, mixing index is calculated on the basis of the following equation:[1]

$$\mathrm{MI} = 1 - \frac{\sqrt{(1/n)\sum (I_i - I_{av})^2}}{I_{av}} \quad (4)$$

where I_i is the fluorescent intensity of each point, I_{av} the average intensity, and n the total number of the pixels. An in-house written Matlab code was used to calculate the mixing index by scanning the fluorescent intensity values over the entire droplet. The mesh of the droplet can be found in SI (Figure S5). Figure 5 shows the effect of the input power on the mixing index for

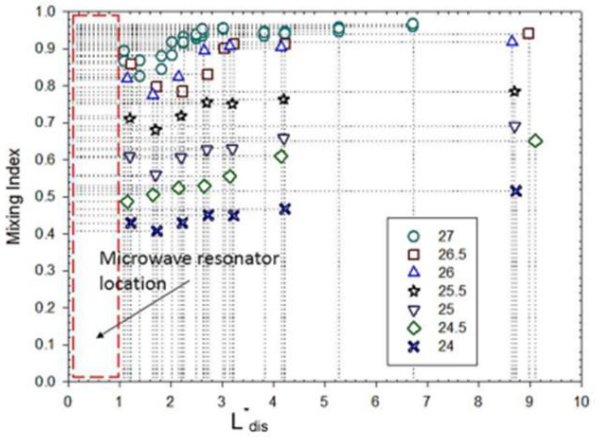

Figure 5. Effect of excitation power (dBm) and L^*_{dis} on mixing efficiency.

75% glycerol solution at the operating frequency of 1.91 GHz, where x-axis is the distance that the droplet traveled after entering the resonator region (the edge of the resonator is marked as x = 0 in Figure 1), which is scaled by the droplet width for ease of comparison. For this particular case, the resonator is 200 μm long, which is reflected by L^*_{dis} = 0−1 in Figure 5. It can be seen that the mixing index increases with the input power for the same distance that the droplet traveled. In this work, with the assistance of fluorescent imaging, a mixing index of 0.8 can be used as a threshold for acceptable mixing though an excellent and thorough mixing is represented by a mixing index of 0.97, which was achieved after the droplet traveled about two droplet widths when the input power is as high as 27 dBm (0.5W). It takes a droplet to travel more than three droplet widths to achieve a mixing index of 0.47 when the input power is reduced to 24 dBm (0.25W). It is also noted

that when the input power is above 26 dBm, no significant benefits by further increasing the input power.

Considering the dominant role of the Marangoni effect in microwave mixing, it is beneficial to obtain a correlation between the mixing index and dimensionless interfacial tension, which could be used for design guidance. Figure 6 shows that

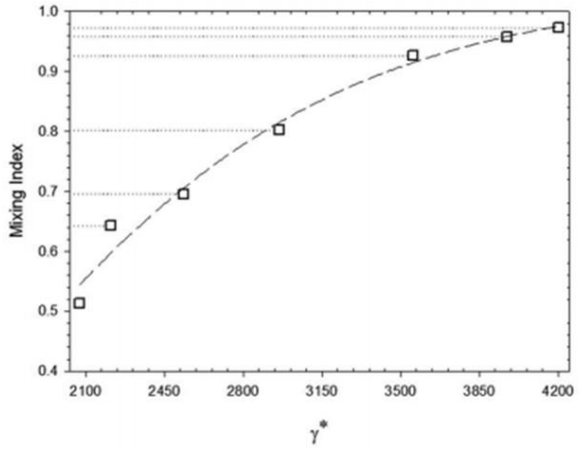

Figure 6. Influence of γ^* on mixing index.

the mixing index increases with the dimensionless interfacial tension which is expected as the higher influence from the interfacial tension, the faster and stronger mixing. A qualitatively critical interfacial tension is observed, $\gamma^* = 3500$, at which the mixing reaches 90%. We obtained an experimental correlation as below,

$$MI = [1 - \exp(-1.226*10^{-3}\cdot\gamma^*)]^{7.654} \quad (5)$$

To further examine our microwave-based microfluidic mixer, mixing within larger droplets (meaning longer droplets as they are confined by the channel width) was also studied. Figure S7 shows effective mixing occurring within droplets of 750 μm long.

CONCLUSIONS

In this study, we demonstrated the mixing capability of a microwave integrated with droplet-based microfluidic devices as a proof-of-concept. In order to shed light on the complex mixing mechanism of a microwave, magnitude analysis of competing forces was performed using the Bukingham Pi theorem. The quantitative evaluation of the mixing index and the effect of the input power and droplet length on the mixing index were also investigated. The mixing platform demonstrated here is simple to integrate with microfluidics, easy to operate, and provides great potential for mixing in many lab-on-a-chip applications that requires rapid and effective mixing. This new mixer may open a new window for mixing biochemical assays on demand. Our mixer can trigger and initiate reactions at the same time of mixing phenomena happening using the microwave energy, while many other mixers can do the mixing function only. This unique approach of utilizing microwave sensor technology to facilitate microfluidics mixing is expected to find wide applications in the field of biochemical synthesis and click-chemistry.

ACKNOWLEDGMENTS

The authors gratefully acknowledge the support from Natural Science and Engineering Council of Canada, Canada Foundation for Innovation, Canada Research Chair program, through grants to Dr. Carolyn L. Ren.

REFERENCES

(1) Ozcelik, A.; Ahmed, D.; Xie, Y.; Nama, N.; Qu, Z.; Nawaz, A. A.; Huang, T. J. *Anal. Chem.* **2014**, *86*, 5083−5088.
(2) Muradoglu, M.; Stone, H. A. *Phys. Fluids* **2005**, *17*, 073305.
(3) Grigoriev, R. O. *Phys. Fluids* **2005**, *17*, 033601.
(4) Grigoriev, R. O.; Schatz, M. F.; Sharma, V. *Lab Chip* **2006**, *6*, 1369−72.
(5) Wen, C.-Y.; Yeh, C.-P.; Tsai, C.-H.; Fu, L.-M. *Electrophoresis* **2009**, *30*, 4179−86.
(6) Chang, C.-C.; Fu, L.-M.; Yang, R.-J. In *Encyclopedia of Microfluidics and Nanofluidics*; Li, D., Ed.; Springer: Berlin, 2015; pp 40−47.
(7) Lee, C.-Y.; Chang, C.-L.; Wang, Y.-N.; Fu, L.-M. *Int. J. Mol. Sci.* **2011**, *12*, 3263−87.
(8) Teh, S.-Y.; Lin, R.; Hung, L.-H.; Lee, A. P. *Lab Chip* **2008**, *8*, 198−220.
(9) Nguyen, N.-T.; Wu, Z. *J. Micromech. Microeng.* **2005**, *15*, R1−R16.
(10) Wang, S.; Huang, X.; Yang, C. *Lab Chip* **2011**, *11*, 2081−7.
(11) Chen, C.-Y.; Chen, C.-Y.; Lin, C.-Y.; Hu, Y.-T. *Lab Chip* **2013**, *13*, 2834−9.
(12) Viefhues, M.; Eichhorn, R.; Fredrich, E.; Regtmeier, J.; Anselmetti, D. *Lab Chip* **2012**, *12*, 485−94.
(13) Salmanzadeh, A.; Shafiee, H.; Davalos, R. V.; Stremler, M. A. *Electrophoresis* **2011**, *32*, 2569−2578.
(14) Cheng, I. F.; Chiang, S. C.; Chung, C. C.; Yeh, T. M.; Chang, H. C. *Biomicrofluidics* **2014**, *8*, 061102.
(15) Sin, M. L. Y.; Shimabukuro, Y.; Wong, P. K. *Nanotechnology* **2009**, *20*, 165701.
(16) Chen, J. K.; Yang, R. J. *Electrophoresis* **2007**, *28*, 975−983.
(17) Lu, L.; Ryu, K. S.; Liu, C. *J. Microelectromech. Syst.* **2002**, *11*, 462−469.
(18) Kang, T. G.; Hulsen, M. A.; Anderson, P. D.; Den Toonder, J. M. J.; Meijer, H. E. H. *Phys. Rev. E* **2007**, *76*, 1−11.
(19) Kitenbergs, G.; Erglis, K.; Perzynski, R.; Cebers, A. *J. Magn. Magn. Mater.* **2015**, *380*, 227−230.
(20) Ganguly, R.; Hahn, T.; Hardt, S. *Microfluid. Nanofluid.* **2010**, *8*, 739−753.
(21) Tsai, J.; Lin, L. *Sens. Actuators, A* **2002**, *97-98*, 665−671.
(22) Xu, B.; Wong, T. N.; Nguyen, N.-T.; Che, Z.; Chai, J. C. K. *Biomicrofluidics* **2010**, *4*, 044102.
(23) Glasgow, I.; Aubry, N. *Lab Chip* **2003**, *3*, 114−120.
(24) Okkels, F.; Tabeling, P. *Phys. Rev. Lett.* **2004**, *92*, 038301.
(25) Yaralioglu, G. G.; Wygant, I. O.; Marentis, T. C.; Khuri-Yakub, B. T. *Anal. Chem.* **2004**, *76*, 3694−3698.
(26) Yang, Z.; Matsumoto, S.; Goto, H.; Matsumoto, M.; Maeda, R. *Sens. Actuators, A* **2001**, *93*, 266−272.
(27) Phan, H. V.; Coskun, M. B.; Sesen, M.; Pandraud, G.; Neild, A.; Alan, T. *Lab Chip* **2015**, *15*, 4206−4216.
(28) Ahmed, D.; Mao, X.; Shi, J.; Juluri, K.; Huang, J. T. *Lab Chip* **2009**, *9*, 2738−2741.
(29) Ahmed, D.; Mao, X.; Juluri, B. K.; Huang, T. J. *Microfluid. Nanofluid.* **2009**, *7*, 727−731.
(30) Nguyen, N.-T. *Micromixers Fundamentals Design and Fabrication*; William Andrew, Inc.: Norwich, NY, 2008.
(31) Kinoshita, H.; Kaneda, S.; Fujii, T.; Oshima, M. *Lab Chip* **2007**, *7*, 338−346.
(32) Malsch, D.; Kielpinski, M.; Merthan, R.; Albert, J.; Mayer, G.; Kohler, J. M.; Suse, H.; Stahl, M.; Henkel, T. *Chem. Eng. J.* **2008**, *135*, S166−S172.
(33) Ma, S.; Sherwood, J. M.; Huck, W. T. S.; Balabani, S. *Lab Chip* **2014**, *14*, 3611.

(34) Boybay, M. S.; Jiao, A.; Glawdel, T.; Ren, C. L. *Lab Chip* **2013**, *13*, 3840−6.
(35) Song, H.; Bringer, M. R.; Tice, J. D.; Gerdts, C. J.; Ismagilov, R. F. *Appl. Phys. Lett.* **2003**, *83*, 4664−4666.
(36) Yesiloz, G.; Boybay, M. S.; Ren, C. L. *Lab Chip* **2015**, *15*, 4008−4019.
(37) Glawdel, T.; Elbuken, C.; Ren, C. L. *Phys. Rev. E* **2012**, *85*, 16322.
(38) Wong, D.; Yesiloz, G.; Boybay, M. S.; Ren, C. L. *Lab Chip* **2016**, *16*, 2192−2197. Stone, Z. B.; Stone, H. A. *Phys. Fluids* **2005**, *17*, 063103.
(39) Stone, Z. B.; Stone, H. A. *Phys. Fluids* **2005**, *17*, 063103.
(40) Cengel, Y. A.; Cimbala, J. M. *Fluid Mechanics: Fundamentals and Applications*; McGraw-Hill Co.: New York, 2006.
(41) Buckingham, E. *Phys. Rev.* **1914**, *4*, 345−376.
(42) White, F. M. *Fluid Mechanics*; McGraw-Hill Co.: New York, 2011.
(43) Braga, J.; Desterro, J. M.; Carmo-Fonseca, M. *Mol. Biol. Cell* **2004**, *15* (10), 4749−4760.
(44) Cordero, M. L.; Rolfsnes, H. O.; Burnham, D. R.; Campbell, P. A.; McGloin, D.; Baroud, C. N. *New J. Phys.* **2009**, *11*, 075033.
(45) Wiggins, S.; Ottino, J. M. *Philos. Trans. R. Soc., A* **2004**, *362*, 937−970.
(46) Li, Y.; Xu, Y.; Feng, X.; Liu, B.-F. *Anal. Chem.* **2012**, *84* (21), 9025−9032.